Downloaded from http://rstb.royalsocietypublishing.org/ on January 16, 2018

The Royal Society

A continuous dynamic beam model for swimming fish

J.-Y. Cheng[1], T. J. Pedley[1]* and J. D. Altringham[2]

[1]*Department of Applied Mathematical Studies and* [2]*Department of Biology, University of Leeds, Leeds LS2 9JT, UK*

When a fish swims in water, muscle contraction, controlled by the nervous system, interacts with the body tissues and the surrounding fluid to yield the observed movement pattern of the body. A continuous dynamic beam model describing the bending moment balance on the body for such an interaction during swimming has been established. In the model a linear visco-elastic assumption is made for the passive behaviour of internal tissues, skin and backbone, and the unsteady fluid force acting on the swimming body is calculated by the 3D waving plate theory. The body bending moment distribution due to the various components, in isolation and acting together, is analysed. The analysis is based on the saithe (*Pollachius virens*), a carangiform swimmer. The fluid reaction needs a bending moment of increasing amplitude towards the tail and near-standing wave behaviour on the rear-half of the body. The inertial movement of the fish results from a wave of bending moment with increasing amplitude along the body and a higher propagation speed than that of body bending. In particular, the fluid reaction, mainly designed for propulsion, can provide a considerable force to balance the local momentum change of the body and thereby reduce the power required from the muscle. The wave of passive visco-elastic bending moment, with an amplitude distribution peaking a little before the mid-point of the fish, travels with a speed close to that of body bending. The calculated muscle bending moment from the whole dynamic system has a wave speed almost the same as that observed for electromyogram-onset and a starting instant close to that of muscle activation, suggesting a consistent matching between the muscle activation pattern and the dynamic response of the system in steady swimming. A faster wave of muscle activation, with a variable phase relation between the strain and activation cycle, appears to be designed to fit the fluid reaction and, to a lesser extent, the body inertia, and is limited by the passive internal tissues. Higher active stress is required from caudal muscle, as predicted from experimental studies on fish muscle. In general, the active force development by muscle does not coincide with the propulsive force generation on the tail. The stiffer backbone may play a role in transmitting force and deformation to maintain and adjust the movement of the body and tail in water.

Keywords: fish; hydrodynamics; muscle activation; muscle mechanics; swimming

1. INTRODUCTION

The lateral movement of a fish body is produced by activation of its muscles. When the fish swims in water, the muscles, controlled by the nervous system, contract in such a way that their interaction with the tissues of the body and the surrounding fluid will result in the observed pattern of body movement and generate the thrust needed to overcome viscous drag. How the body movement in water produces propulsion and how the propulsive performance differs between various swimming modes can be studied by hydrodynamical analysis. Since Lighthill's pioneering work (Lighthill 1960), there has been considerable progress in understanding many aspects of fish hydrodynamics (Wu 1971*a*; Lighthill 1975; Webb & Weihs 1983; Karpouzian *et al.* 1990; Lighthill & Blake 1990).

Recent electromyography experiments on swimming fish (Williams *et al.* 1989; van Leeuwen *et al.* 1990; Kesel *et al.* 1992; Wardle & Videler 1993) have provided the time course of muscle activation (electromyogram (EMG) activity) in relation to bending along the body of swimming fish of various species. It was found that during steady swimming the muscle elements (myotomes) are activated by a wave of motor neuron activity which travels from the head (rostral) towards the tail (caudal). The propagation speed of EMG-onset is somewhat higher than that of the bending wave, whereas that of EMG-termination is much higher, almost a standing wave.

Altringham & Johnston (1990*a*,*b*) studied the power output of fish muscle fibres under locomotory conditions, simulating their activity at different swimming speeds, and investigating the relation between fish size and muscle dynamic behaviour. The properties of muscle fibres in saithe were found to vary along the length of the body, probably to optimize the transmission of power to the tail (Altringham *et al.* 1993; see Wardle *et al.* 1995 for review).

To understand how muscle contraction interacts with the mechanical properties and dynamic processes of the body and surrounding fluid to achieve the required body movements, various theoretical models have been proposed. By using a constitutive relation for sarcomeres,

*Author and address for correspondence: Department of Applied Mathematics & Theoretical Physics, Silver Street, Cambridge CB3 9EW, UK.

Received 8 January 1997 *Accepted* 4 June 1997
© 1998 The Royal Society

Downloaded from http://rstb.royalsocietypublishing.org/ on January 16, 2018

van Leeuwen *et al.* (1990) analysed the function of red muscle at different positions on the body in a swimming carp. The distribution of bending moment required to balance hydrodynamic force and body inertia in a swimming saithe has been studied on the basis of a continuous beam model, with fluid force calculated either by Lighthill's (1971) elongated-body theory (Hess & Videler 1984), or by the 3D waving plate theory for a body shape of uniform depth (Cheng & Blickhan 1994). These studies have made it clear that the observed undulatory motion of a fish in water is produced by a wave of bending moment in the body whose propagation speed is different from, and on average much greater than, that of the lateral undulation wave, though the bending moment wave is not in general a standing wave.

It should be noted that this overall bending moment is not equivalent to the bending moment generated directly by muscle contraction, although that is the only power source for fish swimming. The body bending is also subject to mechanical constraints imposed by the internal structure. Hebrank (1982) has studied the role of the backbone in fish swimming, and suggested that the mechanical properties of the backbone are tuned to fit the particular swimming modes used. The functions of fish skin during body bending for locomotion have been studied by Wainwright *et al.* (1978) for the shark, and by Hebrank (1980) for the eel. They suggested that the skin, composed largely of a crossed-helical array of fibres, may act as an external tendon to transmit the force of muscle contraction and displacement down the length of the fish. In general, all skeletal elements within the body, such as connective tissues, skin and backbone, and passive muscle fibres themselves, are subjected to deformation during swimming and therefore generate stresses which oppose that deformation. The bending of the body will therefore be modified or limited by their dynamic properties. The dynamic effect of all elements of the body when they experience strain must be considered in modelling body dynamics for swimming fish. Bowtell & Williams (1991) have proposed a discrete dynamic model for the lamprey, including tissue mechanics represented by a number of springs and dashpots but without consideration of the fluid reaction. They have subsequently improved their model by allowing continuous deformation of the body (Bowtell & Williams 1993).

In this paper we propose a continuous beam model for a swimming fish, describing the interaction of muscle contraction with all the body tissues and the surrounding fluid. From the fish's point of view, input to the swimming process is the signal that propagates along the spinal cord, activating the muscles alternately on either side of the fish. At any instant, a muscle contracts at a rate determined by its current length, the level of activation, the load against which it is contracting, and its past history. The load comes from the visco-elastic properties of the fish body, its inertia, and the hydrodynamics. The fish integrates all these features to produce the observed wave of bending.

However, input to our model must be something measurable, and the easiest quantity to measure is the wave of displacement of the fish's median surface from a flat plane (Videler & Hess 1984; Wardle & Videler 1993). We used as input the observed wave of body displacement (or bending) in the saithe, a carangiform swimmer for which as much data are available as for any other species, from Videler & Hess (1984). Then we worked both outwards, analysing the hydrodynamics to compute the load exerted on the fish surface by the water, and inwards, analysing the visco-elastic stresses in the body.

As in almost all studies of fish hydrodynamics (Lighthill 1960, 1971, 1975; Wu 1971*a*; Cheng *et al*. 1991), we conceptually separate the production of thrust, by the essentially non-viscous reaction of the water to lateral movements of the body, from the countervailing drag generated by longitudinal inertia (mass × acceleration), so if we can use the observed motions to calculate the thrust and longitudinal acceleration, we can infer the drag. However, in this paper we are concerned not with the overall thrust and drag but with the time-varying distribution of lateral forces along the body, because it is these that are generated by the bending of the body and that contribute to the distribution of bending moment. In the present small-amplitude model we are justified in neglecting the small contribution that the longitudinal viscous stresses may make to the bending moment distribution (Wu 1971*b*; Hess & Videler 1984).

A further (commonly made) assumption of the hydrodynamic part of our model is that the fish is swimming at a constant speed U. Although the calculated thrust varies during 'steady' swimming, from close to zero to about twice its mean value, the corresponding fluctuations in velocity have been estimated by Hess & Videler (1984), taking into account body inertia as well as drag, as only $\pm 2\%$, so we neglect them. We use the 3D waving plate theory of Cheng *et al.* (1991), rather than Lighthill's elongated-body theory (1975), because, although it is as yet restricted to small amplitude displacement waves, it does not neglect the feedback from the vortex wake onto the fish and appears to be more accurate in the sense that it requires less 'recoil correction' (see § 3; Cheng *et al.* 1991).

The solid-mechanics part of our model is explained in the following sections. In short, we follow Hess & Videler (1984) in showing how the transverse hydrodynamic forces, together with fish body inertia, combine to require the generation of a certain distribution of bending moment by the fish.

The new aspect of our model is to separate that bending moment into contributions from the passive mechanical properties of the (visco-elastic) tissues and from the active contraction of the muscles. Linear visco-elastic properties are assumed for the internal tissues, skin and backbone. We found that, although these properties are important, the precise values of the corresponding parameters are not critical in determining at least the muscle activation pattern, as long as they are taken to lie in a realistic range.

2. THEORETICAL MODEL

(a) *Free beam model for a fish swimming in water*

In a moving system of coordinates (x,y,z), with the origin attached to the anterior tip of the fish, the fluid far away moves in the positive x direction. The longitudinal axis, x, passes through the centre of the cross-section of the body (i.e. the backbone) when the fish is straight and unloaded. The mean surface of the undulating fish is situated in the

Downloaded from http://rstb.royalsocietypublishing.org/ on January 16, 2018

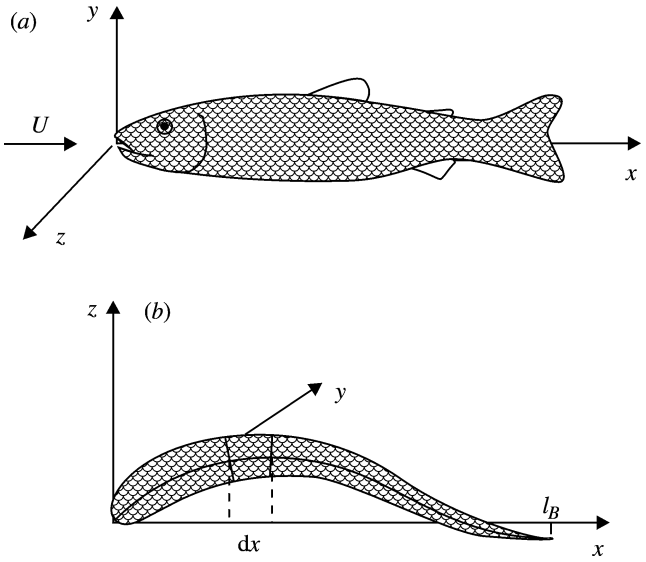

Figure 1. Coordinate system for swimming fish. (*a*) Schematic side view of fish. (*b*) Schematic dorsal view of fish and an arbitrary longitudinal segment of the body.

xy plane and the *z*-axis is in the lateral undulating direction (figure 1).

The lateral movement of the median surface may be taken as

$$z = h(x,y,t) \quad (x,y \in S), \tag{1}$$

where S is the projected area of the median surface on the *xy* plane. At present we do not consider spanwise (dorso-ventral) deformation, so $\partial h/\partial y = 0$. This is realistic for most fish movement except for some parts of the tail or extended fins.

In our model, we treat the fish as a free beam undergoing small amplitude bending oscillations. The lateral bending is caused by the muscle contractile force, but it is also influenced by inertial, viscous and elastic forces due to all the tissues within the fish body as well as by the surrounding fluid. If the cross-sectional area of the body at distance x from the nose is denoted as $g(x)$, an arbitrary infinitesimal segment of the fish has volume $g(x)\mathrm{d}x$ (figure 1*b*). The forces and moments acting on this segment are shown in figure 2. We can write down the dynamic equation for this segment as follows (Cheng & Blickhan 1994),

$$\frac{\partial T_q}{\partial x} + Q = 0, \tag{2}$$

$$-\frac{\partial F}{\partial x} + L_y - D = m_b(x)\frac{\partial^2 h}{\partial t^2} - \frac{\partial}{\partial x}\left(T_q \frac{\partial h}{\partial x}\right), \tag{3}$$

$$-F - \frac{\partial M}{\partial x} = 0, \tag{4}$$

where $m_b(x)$ is the mass of the body per unit length, $Q(x,t)$ is the longitudinal component of fluid shear and pressure forces per unit length, $T_q(x,t)$ is the longitudinal tension induced by Q, $L_y(x,t)$ is the lateral force exerted by the water per unit length (i.e. the spanwise integrated pressure difference across the body), $D(x,t)$ is the transverse viscous

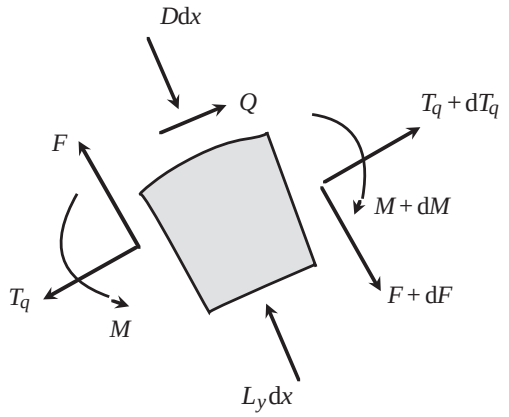

Figure 2. Forces and moments acting on a longitudinal volume element $g(x)\mathrm{d}x$ (hatched) of a fish body.

drag per unit length, $F(x,t)$ is the shear force in a cross-sectional plane, and $M(x,t)$ is the net bending moment.

Q, T_q and D are normally small compared with the other quantities for a fish which varies slowly along its length, swimming at large Reynolds numbers, provided there is no separation of the flow around the body. So terms associated with those quantities may be ignored in the above equations. Then, (2), (3) and (4) become

$$\frac{\partial^2 M}{\partial x^2} = -L_y + m_b(x)\frac{\partial^2 h}{\partial t^2}, \tag{5}$$

as derived by Hess & Videler (1984). The boundary conditions are that the shear force $F(x,t)$ and bending moment $M(x,t)$ vanish at the free ends, giving

$$M = \frac{\partial M}{\partial x} = 0 \quad \text{at } x = 0, l_B, \tag{6}$$

where l_B is the body length. This means that there are four conditions to be applied to the solution of a second order differential equation (5). That is not normally possible; the requirement that they should be satisfied imposes a constraint on the form of the function $h(x,t)$. This leads to the so-called 'recoil correction', which is further discussed in § 3.

During body bending the contractile elements (cross-bridges) of each muscle generate an active force which is related to the length of the fibre and the rate of shortening (Hill 1938). The collective action of all of the filaments at position x generates a bending moment $M_m(x,t)$: this in turn is modulated by the passive properties of the fish body, which make a further contribution, M_p, to the bending moment. The total bending moment M may thus be written as a combination of these two contributions:

$$M = M(M_m, M_p), \tag{7}$$

where the active bending moment M_m is caused by muscular contractions which produce the time-varying tension and compression, and are resisted by the passive bending moment M_p due to the mechanical properties, elastic and viscous, of the enclosed tissues.

(b) *Strain in the body*

Now we consider the strain in the body produced by pure bending. Here small deformations of the body are assumed so that the problem can be linearized. For large

Downloaded from http://rstb.royalsocietypublishing.org/ on January 16, 2018

amplitude manoeuvres a large-strain analysis (van Leeuwen *et al.* 1990) may be required, but the lack of pertinent data makes that inappropriate at this stage.

Because no spanwise variations of any quantities are assumed, the following description will be based on deformations in the xz plane. For the volume segment shown before bending in figure 3*a*, we choose straight line segments x_1x_2 and x_3x_4, which correspond to the xy plane and a plane parallel to the xy plane, respectively. After bending caused by the bending moment M in the cross-sectional plane, x_1x_2 and x_3x_4 are changed into curved segments $x'_1x'_2$ and $x'_3x'_4$ (figure 3*b*). It is assumed that there is a neutral curve, corresponding to the median surface of the body, i.e. the backbone, whose length does not change. The slope at an arbitrary point on the neutral curve, relative to the x-axis, is denoted by θ. If we assume that during bending the originally plane cross-sections of the body remain plane and perpendicular to the backbone, then the lines $x'_3x'_1$ and $x'_4x'_2$ are both on radii of curvature. The centre of curvature is at their intersection C where the angle subtended is $\mathrm{d}\phi$. The radius of curvature of the surface through $x'_1x'_2$ is denoted by R.

We assume that the only normal stresses acting on a cross-section are those caused by muscle contraction and the passive mechanical response of the tissues. These internal stresses have as their resultant the bending moment M. It is expected that part of the cross-section will be in tension and part in compression (figure 3*c*). The neutral surface of zero stress, for example the median surface through $x'_1x'_2$, separates these zones. From figure 3*b* we have

$$x_1x_2 = x'_1x'_2 = \mathrm{d}x = R\mathrm{d}\phi,$$

$$x_3x_4 = \mathrm{d}x = R\mathrm{d}\phi,$$

$$x'_3x'_4 = (R+z)\mathrm{d}\phi,$$

so the normal strain in the x direction is,

$$\epsilon = \frac{(R+z)\mathrm{d}\phi - R\mathrm{d}\phi}{R\mathrm{d}\phi} = \frac{z}{R}, \tag{8}$$

which shows that the normal strain is directly proportional to the distance from the neutral surface. Such a theoretical description of the normal strain, in principle, agrees with the real case for which deeper muscle fibres are presumed to undergo smaller strains (Alexander 1969; Rome & Sosnicki 1991).

For an arbitrary infinitesimal segment $\mathrm{d}s$ which corresponds to the positive bending moment (figure 3*b*), the angle at x'_1 is θ and at x'_2 is $(\theta - \mathrm{d}\phi)$. Therefore,

$$\frac{1}{R} = \frac{\mathrm{d}\phi}{\mathrm{d}s} = -\frac{\mathrm{d}\theta}{\mathrm{d}s}, \tag{9}$$

as a positive increment $\mathrm{d}s$ in figure 3*b* is associated with a reduction of θ by $\mathrm{d}\phi$ i.e. $\mathrm{d}\phi = -\mathrm{d}\theta$. Because we assume a small amplitude movement, then

$$\mathrm{d}x = \mathrm{d}s\cos\theta \approx \mathrm{d}s, \tag{10}$$

and

$$\theta \approx \tan\theta = \frac{\partial h}{\partial x}, \tag{11}$$

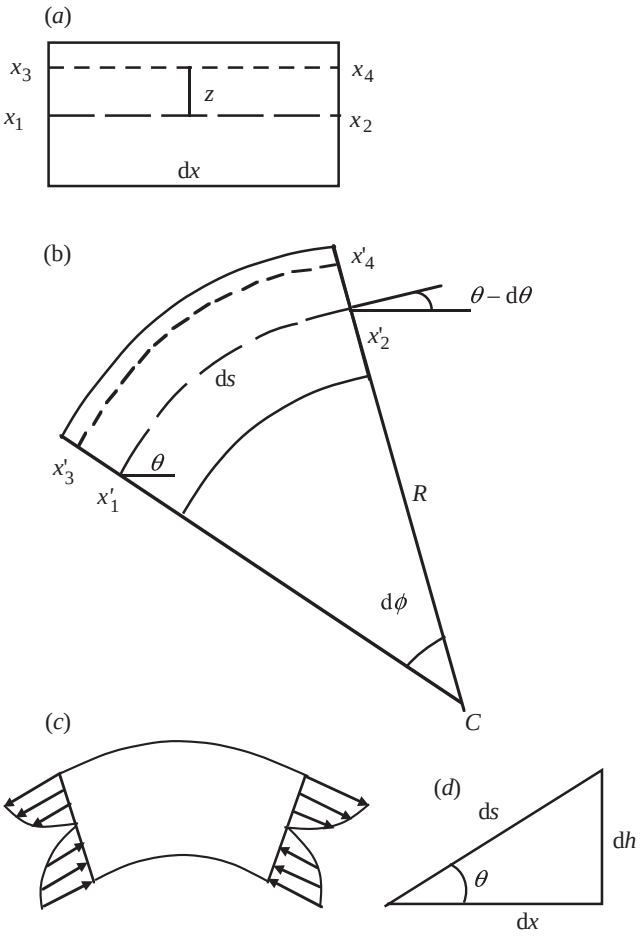

Figure 3. An infinitesimal longitudinal segment of a fish body: (*a*) geometry before bending; (*b*) geometry after bending; (*c*) stress state after bending. (*d*) Sketch relating $\mathrm{d}h$, $\mathrm{d}s$, $\mathrm{d}x$ and θ.

and we have

$$\frac{1}{R} = -\frac{\partial\theta}{\partial x} = -\frac{\partial}{\partial x}\frac{\partial h}{\partial x} = -\frac{\partial^2 h}{\partial x^2}, \tag{12}$$

where h is the lateral displacement (equation (1)).

(c) *Visco-elastic assumption for passive elements in the body*

An important feature of the model, in principle, is the the constitutive relation between stress and strain for the tissues of the fish body. The structural and mechanical features of all tissues may conform to, or limit, the locomotor bending. Most elements within the fish body, such as septa, skin and backbone, may transmit force and deformation from the muscle to the caudal fin, and participate in the bending of the body (Wainwright 1984). As quantitative information on the mechanical properties of these elements is scarce, some basic assumptions about the constitutive behaviour of biomaterials in fish have to be made.

In general, it is expected that all structural biomaterials in the fish will have some viscous behaviour because they are hydrated, and all materials are also more or less elastic. The stiffest materials in the fish are likely to be bone or calcified cartilage. At first we assume that the fish body consists of several types of visco-elastic material.

Downloaded from http://rstb.royalsocietypublishing.org/ on January 16, 2018

At this stage it is reasonable to suppose that the power unit, elastic unit and damping unit are arranged in a parallel manner for an arbitrary body segment, and experience the same strain ($d\theta$) during bending (Bowtell & Williams 1991). Then the bending moment due to muscle contraction, and the elasticity and viscosity of the tissues, should be added together. This arrangement is similar to a Voigt model in visco-elasticity theory (Fung 1981). We thus have

$$M = M_m + M_p = M_m + M_e + M_v, \tag{13}$$

where M_e and M_v are the bending moments due to passive elasticity and viscosity, respectively.

Unstimulated passive tissues are represented by simple constitutive models. Assuming a linearly elastic and viscous material, we have

$$\sigma_e = E\epsilon = E\frac{z}{R}, \tag{14}$$

$$\sigma_v = \mu\frac{\partial\epsilon}{\partial t} = \mu z\frac{\partial}{\partial t}\left(\frac{1}{R}\right), \tag{15}$$

where σ_e and σ_v are the normal stress on the cross-section due to the passive elasticity and viscosity, respectively, E is the Young's modulus and μ is the viscosity coefficient of the tissue.

The bending moments caused by the elasticity and viscosity at any position along the x-axis are thus

$$M_e = \int_A z\sigma_e dA = \frac{1}{R}\int_A E(y,z)z^2 dA = \frac{\overline{E}I}{R}, \tag{16}$$

$$M_v = \int_A z\sigma_v dA = \frac{\partial}{\partial t}\left(\frac{1}{R}\right)\int_A \mu(y,z)z^2 dA = \overline{\mu}I\frac{\partial}{\partial t}\left(\frac{1}{R}\right), \tag{17}$$

where E and μ are variable over the cross-section A, so they cannot be taken outside the integrations. In our beam model for the bending of the fish body, the roles of the elasticity and viscosity are reflected by the combined parameters $\overline{E}I$ and $\overline{\mu}I$, which may be called the elastic and viscous bending moduli, respectively. They are the second moments of area of the cross-section about the y-axis weighted by E and μ, respectively, and depend on the distribution of materials in the cross-section, and the shape and dimensions of the section.

Looking at a typical cross-section, we see that the body is composed of different biomaterials. We can roughly divide the cross-section into three regions, excluding the head and tail (figure 4).

1. The inner vertebral column region with constants E_1 and μ_1.
2. The intermediate region of muscle and other tissues with constants E_2 and μ_2.
3. The outer skin region with constants E_3 and μ_3.

Obviously, the mechanical properties of the three regions may be quite different. In the present model, it is assumed, in the absence of quantitative data, that the material properties of each region are independent of location along the fish.

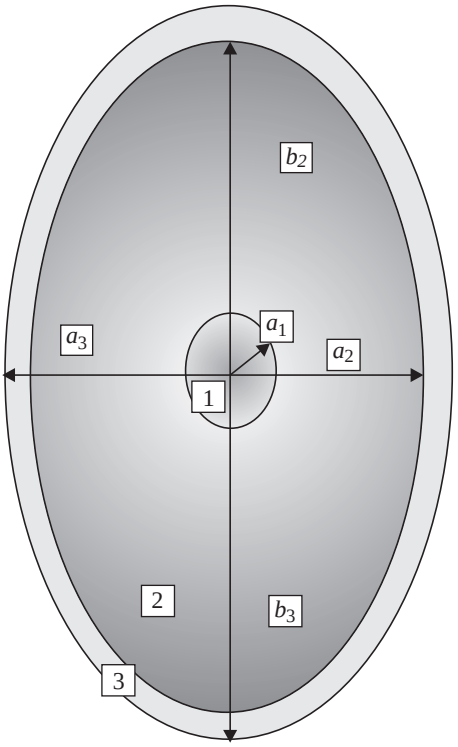

Figure 4. Cross-section of fish body, divided into three regions: 1, backbone; 2, muscle and other tissues; and 3, skin.

If the three regions are assumed to be uniform, the weighted second moment of area of each region is the product of its second moment of area and its constant weight. The two integrals can then be replaced by two summations, i.e.

$$\overline{E}I = \sum_{i=1}^{3} E_i I_i,$$
$$\overline{\mu}I = \sum_{i=1}^{3} \mu_i I_i. \tag{18}$$

It is reasonable to take the cross-sections of the fish body to be elliptical, and the backbone to be circular (still excluding the head). Referring to figure 4, the radius of region 1 is taken as a_1, the lengths of the semi-axes of the ellipses corresponding to regions 2 and 3 as a_2, b_2, and a_3, b_3, respectively. We thus have

$$I_1 = \frac{\pi}{4}a_1^4,\ I_2 = \frac{\pi}{4}(a_2^3 b_2 - a_1^4),\ I_3 = \frac{\pi}{4}(a_3^3 b_3 - a_2^3 b_2). \tag{19}$$

Furthermore, we suppose that

$$a_1 = \frac{1}{N}a_{3m},\ a_2 = a_3 - \Delta h,\ b_2 = b_3 - \Delta h, \tag{20}$$

where a_{3m} is the maximum value of a_3, Δh is the constant skin thickness, and $N(x)$ is a given function of x. For the head ($x \leqslant x_h$) it is assumed that only region 1 exists, so we have

$$I_2 = 0, I_3 = 0,\ x \leqslant x_h. \tag{21}$$

The normal stress owing to both viscosity and elasticity is

$$\sigma_{pi} = \sigma_{ei} + \sigma_{vi} = \frac{zE_i}{EI}M_e + \frac{z\mu_j}{\overline{\mu}I}M_v,\ i = 1,2,3. \tag{22}$$

Downloaded from http://rstb.royalsocietypublishing.org/ on January 16, 2018

In general, σ_p varies with z and, through the load M_e and M_v, and the body shape parameter I_i, with x.

(d) *Stress caused by muscle contraction*

In principle, a mathematical model describing the active dynamic properties of fish muscle could be established following the work of van Leeuwen *et al.* (1990), Altringham & Johnston (1990*a*,*b*) and Altringham *et al.* (1993). Here, however, we will not go into so much detail. If the active muscle bending moment required by the entire system during body bending can be determined, the muscle stress distribution may be approximately calculated from it. Denoting the active muscle stress as σ_m which is distributed over an area A_m of the cross-section, the bending moment produced by it about the y-axis is

$$M_m = \int_{A_m} z\sigma_m \mathrm{d}A. \tag{23}$$

At any instant, only one side of the fish is activated while the other side is passively deformed. We may therefore suppose the active muscle force exists on one side and is equal to zero on the other, for example,

$$\sigma_m = \begin{cases} \sigma_m & z > 0 \\ 0 & z < 0. \end{cases} \tag{24}$$

If we take σ_m as constant, equal to the average value over the area $A_m/2$, to simplify the integral (23), then we can calculate the stress σ_m from the muscle bending moment, i.e.

$$\sigma_m = \frac{M_m}{\mathcal{J}}, \tag{25}$$

where $\mathcal{J} = \int_{A_m/2} z\mathrm{d}A$ is the first moment of area $A_m/2$ about the z-axis. Thus, in general, σ_m varies with x through M_m and also depends on the cross-section through $\mathcal{J}$.

The active muscle region A_m may be that occupied by slow or fast muscle, or both. In steady-swimming slow-muscle fibres, which lie as a thin strip directly underneath and parallel to the skin along the lateral line, could be responsible for force generation as observed in carp by van Leeuwen *et al.* (1990). In the saithe, superficial fast fibres are recruited at around 5 Hz during steady swimming (Altringham *et al.* 1993), close to the frequency of 4 Hz to be used here from Videler & Hess (1984). It is probable that at low sustainable speeds only the most superficial fast fibres, close to the slow ones, will be active. As speed increases, deeper fast fibres will be recruited. What proportion of area 2 is used at 5 Hz is unknown: at 4 Hz it is likely to be very small. When the fast muscle fibres are active during rapid steady swimming, A_m will be close to the area of region 2 in figure 4 and $\mathcal{J} = \frac{2}{3}\left(a_2^2 b_2 - a_1^3\right)$.

(e) *Dynamic equation*

From (12), (16) and (17) we have

$$M_e = -\overline{E}I\frac{\partial^2 h}{\partial x^2}, \tag{26}$$

$$M_v = -\overline{\mu}I\frac{\partial}{\partial t}\frac{\partial^2 h}{\partial x^2}, \tag{27}$$

and

$$M = M_m - \overline{E}I\frac{\partial^2 h}{\partial x^2} - \overline{\mu}I\frac{\partial}{\partial}\frac{\partial^2 h}{\partial x^2}. \tag{28}$$

Substituting (28) into (5), we have the differential equation governing the dynamic system:

$$\frac{\partial^2 M_m}{\partial x^2} - \frac{\partial^2}{\partial x^2}\left[\overline{E}I\frac{\partial^2 h}{\partial x^2}\right] - \frac{\partial^2}{\partial x^2}\left[\overline{\mu}I\frac{\partial}{\partial t}\frac{\partial^2 h}{\partial x^2}\right] + L_y - m_b(x)\frac{\partial^2 h}{\partial t^2} = 0. \tag{29}$$

If we denote

$$L_y = \frac{\partial^2 M_h}{\partial x^2}, \quad -m_b(x)\frac{\partial^2 h}{\partial t^2} = \frac{\partial^2 M_i}{\partial x^2}, \tag{30}$$

where M_h and M_i are the contributions to the bending moment from the hydrodynamic and inertial forces, respectively, then we have

$$\frac{\partial^2}{\partial x^2}\left(M_m + M_e + M_v + M_h + M_i\right) = 0. \tag{31}$$

This equation represents a dynamic system for the swimmer's body constructed from a power source M_m, stiffness unit M_e, damping unit M_v, fluid reaction M_h, and body inertia M_i. How the fish controls, and the system allows, swimming behaviour may be studied by considering the interaction of all elements of the system. This is a solid–fluid interaction problem, and in general an iterative approach needs to be taken. Our approach is to take the observed movements of the swimming fish as input, and use them: (i) to calculate the relative water motion and the hydrodynamic loading, and hence M_h; (ii) then compute the inertial contribution M_i; and (iii) to estimate the passive contributions M_e and M_v as outlined above. Then the muscle bending moment M_m is calculated from equation (31). We may call the problem to be solved by this approach the 'bending moment problem'. Alternatively, we could use the EMG measurement on swimming fish and some kind of constitutive model for the contractile elements (e.g. Hill's equation (Hill 1938) with the constants obtained from experiments on isolated muscle fibres) to infer M_m and input it to the dynamic equation (29) to predict the swimming movement $h(x,t)$ (the 'movement problem'), as suggested by Daniel *et al.* (1992). A comparison between the distribution of $M_m(x,t)$ obtained in this way with that obtained from the bending moment problem should lead to new physiological information about the critical constitutive parameters (such as $\overline{E}, \overline{\mu}$ and muscle properties) and the ranges within which their values should lie.

3. WAVING MOTION, HYDRODYNAMIC METHOD AND RECOIL CORRECTION

The lateral motion of a steadily swimming fish is generally periodic with respect to time. Thus the function $h(x,t)$ in equation (1) can be represented by a Fourier series. Furthermore, the EMG studies of Wardle & Videler (1993) have shown that the muscle activation frequency is the same as the undulation frequency. This suggests that it is appropriate for us to use a single frequency oscillation as

Downloaded from http://rstb.royalsocietypublishing.org/ on January 16, 2018

input to our linear dynamic model (Hess & Videler 1984). Hence, we put

$$h(x,t) = h_1(x)\cos\omega(t - \tau_h(x)), \tag{32}$$

where $h_1(x)$ and $\tau_h(x)$ are the amplitude and phase functions, respectively, $\omega = 2\pi/T_t$ is the angular frequency, and T_t is the time period of the undulation.

If the undulation propagates along the body with a constant wave speed V, (32) becomes

$$h(x,t) = h_1(x)\cos\omega[t - (x/V + \tau_0)], \tag{33}$$

where τ_0 is a constant determined by the definition of the time origin. From (33) we have

$$\frac{\partial^2 h}{\partial x^2} = h_{xx1}(x)\cos\omega[t - \tau_{hxx}(x)], \tag{34}$$

where

$$h_{xx1}(x) = \left\{\left[h_1'' - \left(\frac{\omega}{V}\right)^2 h_1\right]^2 + \left[2\left(\frac{\omega}{V}\right)h_1'\right]^2\right\}^{1/2},$$

$$\tau_{hxx}(x) = \frac{1}{\omega}tg^{-1}\left[\frac{2(\omega/V)h_1'}{h_1'' - (\omega/V)^2 h_1}\right] + \left(\frac{1}{V}x + \tau_0\right).$$

As derived above (equation (12)), $(\partial^2 h/\partial x^2)^{-1}$ is equal to the radius of curvature provided $\partial h/\partial x$ is small, and this will be used to calculate the passive bending moment. It has been found that the displacement amplitude $h_1(x)$ is close to an exponential function of x for many fishes, which ensures that the lateral curvature wave has the same constant wave speed as the lateral displacement wave (Cheng & Blickhan 1994).

As stated in § 1, we assume that the fish swims at constant speed, U, along a rectilinear path. The fish is treated as an undulating plate corresponding to the median surface of the body, and calculation of the unsteady hydrodynamic forces acting on the body is made by applying 3D waving plate theory (Cheng *et al.* 1991). The theory has previously been used to estimate the bending moment distribution without considering the internal tissues (Cheng *et al.* 1993; Cheng & Blickhan 1994). Recently, the theory has been improved to enable more realistic shapes for the whole fish body or for a single fin to be modelled, and it has been employed to study the morphological adaptation of the necking at the peduncle (J.-Y. Cheng, unpublished observation). The measured real outline of a fish can be input directly to calculations of the desired quantities.

The real motion of a fish in water should satisfy the recoil condition, or equivalently the end condition (6), to the effect that the net lateral force and torque provided by hydrodynamic forces on the whole fish should be equal to the rate of change of its lateral translational and angular momentum, respectively (Hess & Videler 1984; Cheng & Blickhan 1994). Because of errors in our dynamic model and in the assumed or measured lateral motion $h(x,t)$ and mass distribution $m_b(x)$, and, more significantly, to inaccuracies in the theory used to calculate the hydrodynamic force, the end condition (6) might not be satisfied. To obtain a net bending moment distribution $M(x,t)$ satisfying equation (6) the motion $h(x,t)$ would have to be modified by adding a rigid-body translation and rotation of the whole body, the recoil $h_s(x,t)$, and so the modified motion is

$$h_{rc}(x,t) = h(x,t) + h_s(x,t) \tag{35}$$

where

$$h_s(x,t) = A(t) + B(t)x. \tag{36}$$

Because of the linearity of the problem, A and B can be determined by using equation (6) and the corresponding bending moment is calculated for the motion $h_{rc}(x,t)$.

It has been found that the recoil correction required by the waving plate theory is much smaller than that required by the elongated-body theory (Cheng & Blickhan 1994). As recoil rotation leads to undesirable energy loss (through vortex shedding from the top and bottom of the body as it moves sideways), which would presumably be minimized in the course of evolution, it seems reasonable to regard the 3D waving plate theory as better than the elongated-body theory in the calculation of the unsteady fluid force on the fish.

Because the bending moment due to the visco-elasticity is given by the curvature of the median surface and its rate of change, a rigid body motion makes no contribution to M_p. The recoil correction process (Cheng & Blickhan 1994) made in calculating the total bending moment is also not influenced by introducing M_p.

4. NON-DIMENSIONALIZATION

The body length l_B, undulation period T_t and water density ρ are chosen as the reference length, time and density to non-dimensionalize all quantities. It is convenient to reformulate the relevant equations in terms of complex variables. Because of the linearity of the problem, all quantities such as the lateral displacement, lateral hydrodynamic force, bending moment and normal stress may be written in complex form as

$$h(x,t) = Re[\tilde{h}(x)\,e^{i\omega t}] = h_1(x)\cos\omega[t - \tau_h(x)], \tag{37a}$$

$$L_y(x,t) = q\Delta C_{py} = qRe[\Delta\tilde{C}_{py}(x)e^{i\omega t}] = q\Delta C_{py1}\cos\omega[t - \tau_L(x)], \tag{37b}$$

$$M(x,t) = Re[\tilde{M}(x)e^{i\omega t}] = M_1(x)\cos\omega[t - \tau_m(x)], \tag{37c}$$

$$\sigma(x,z,t) = Re[\tilde{\sigma}(x,z)e^{i\omega t}] = \sigma_1(x,z)\cos\omega[t - \tau_\sigma(x)], \tag{37d}$$

where Re means 'taking the real part of', ΔC_{py} is the coefficient of pressure difference across the body, $q = 1/2\rho U^2$ is the dynamic pressure, and the angular frequency ω is equal to 2π. Using these dimensionless variables, (5) or (29) become

$$\frac{\partial^2\tilde{M}(x)}{\partial x^2} = -\frac{1}{2}\rho U^2\Delta\tilde{C}_{py}(x) - 4\pi^2 m_b(x)\tilde{h}(x), \tag{38}$$

and

$$\tilde{M} = \tilde{M}_m + \tilde{M}_p, \tag{39}$$

Downloaded from http://rstb.royalsocietypublishing.org/ on January 16, 2018

$$\tilde{M}_{\mathrm{p}} = -\chi I \frac{\partial^2 \tilde{h}(x)}{\partial x^2}, \tag{40}$$

where $\chi = (E + \mathrm{i}2\pi\mu)$ may be called the complex visco-elastic modulus, and χI the corresponding bending modulus. The complex amplitude of the normal stress due to the passive mechanical properties is then

$$\tilde{\sigma}_{\mathrm{p}} = \tilde{\sigma}_{\mathrm{e}} + \tilde{\sigma}_{\mathrm{v}} = -\chi z \frac{\partial^2 \tilde{h}}{\partial x^2} = \frac{\chi z}{\chi I} \tilde{M}_{\mathrm{p}}. \tag{41}$$

The boundary conditions require

$$\frac{\partial \tilde{M}(x)}{\partial x} = \tilde{M}(x) = 0, \quad \text{at } x = 0,1. \tag{42}$$

$\Delta C_{\mathrm{p}y}(x)$ in (38) is calculated from the waving plate theory in which a reduced frequency γ and a wave number k are used; they are defined by

$$\gamma = \frac{\omega l_{\mathrm{B}}}{U} = \frac{2\pi}{U'}, \; k = \frac{2\pi l_{\mathrm{B}}}{\lambda} = \frac{2\pi}{V'}, \tag{43}$$

where U' and V' are dimensionless forms of the swimming speed and wave speed normalized by l_{B} and T_t (λ is the wavelength).

5. KINEMATIC AND DIMENSION PARAMETERS FOR SWIMMING SAITHE

The data given in the literature for the saithe (Videler & Hess 1984; Wardle & Videler 1993) are used to calculate the bending moment distribution along the fish. The measured amplitude distribution of the movement for an 'average' saithe is used as plotted in figure 9. The quantities were averaged from all sequences in the experiments. As the measured movement of the head was not accurate (Videler & Hess 1984), the calculation results for this part may not be meaningful and analysis will be focused on the remainder of the body. The measured distribution of body mass per unit length of the saithe is taken from fig. 3*b* of Hess & Videler (1984). Table 1 lists some body dimensions and kinematic data on 'average' saithe. The wave speed, V (or the wavelength, λ), measured for the posterior half of the fish (the value for the whole body is also listed in table 1) is chosen in our calculations. The side outline of the saithe in fig. 3 of Hess & Videler (1984) is taken for the shape of the waving plate. The influence of this shape on swimming propulsion and dynamics is discussed elsewhere (J.-Y. Cheng, unpublished observations).

We need to know the skin thickness and backbone radius for the saithe. The only data available on skin thickness are for eels: a 20-cm long elver had skin 150–180-μm thick and a 56-cm long adult eel had skin 500–530-μm thick (Hebrank 1980). Accordingly, a skin thickness of 500 μm is assumed for adult saithe: the non-dimensional value is 0.00125. The ratio of skin thickness to maximum half-width of the saithe is

$$\frac{\Delta h}{a_{3\mathrm{m}}} = 0.019 \approx 2 \times 10^{-2}. \tag{44}$$

As the dimension of the cross-section of the backbone normally decreases towards the tail, the ratio of the maximal half-width of the body to the radius of the backbone is taken as 5 at $x = 0.2$, increasing to 7 before the tail.

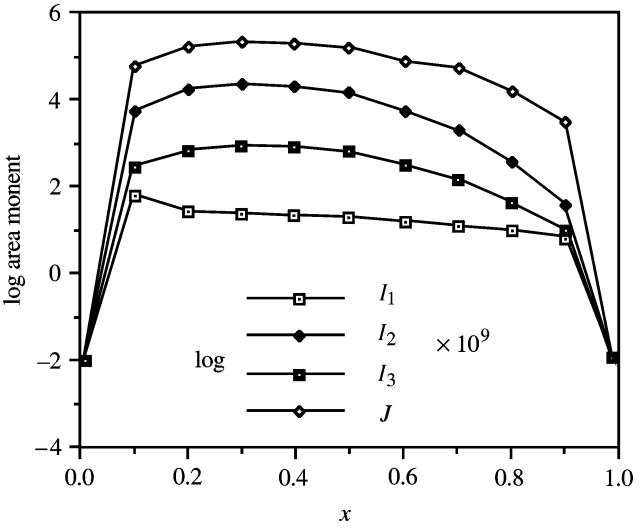

Figure 5. The distribution of area moments of cross-section along the body length in three regions. I_1. I_2 and I_3: the second moments of regions 1, 2 and 3. $\mathcal{J}$: the first moment of half the cross-section of region 2. Note that the left-hand scale is logarithmic.

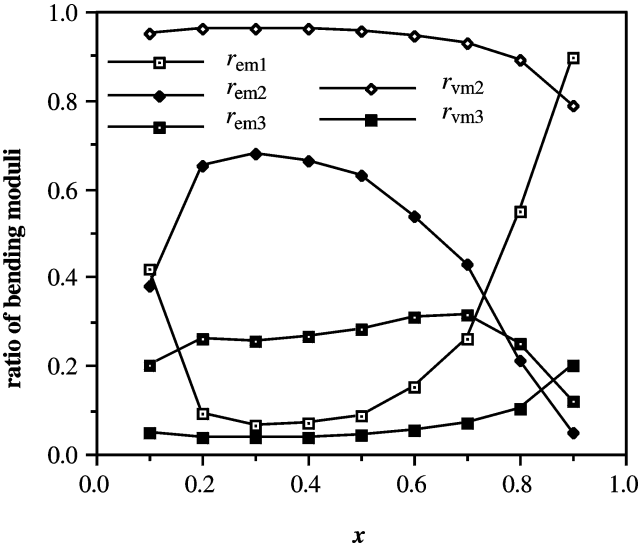

Figure 6. The ratio of the viscous and elastic bending moduli of each region to the total bending modulus of the whole cross-section against distance along the body. r_{em1}, r_{em2} and r_{em3}: the ratio of elastic bending moduli of regions 1, 2 and 3; r_{vm2} and r_{vm3}: the ratio of viscous bending moduli of regions 2 and 3.

6. ESTIMATION OF VISCO-ELASTIC COEFFICIENTS

To use the present dynamic model we need to know quantitatively the mechanical properties of all bio-materials within the fish body. However, there are almost no available data for the saithe. Even for other fishes, the available data are scarce. At present, we have to estimate the visco-elastic parameters of the skin, backbone and muscle for saithe on the basis of very limited information.

Considering the internal complexity of the fish body, the division of the cross-section into three regions is very

Downloaded from http://rstb.royalsocietypublishing.org/ on January 16, 2018

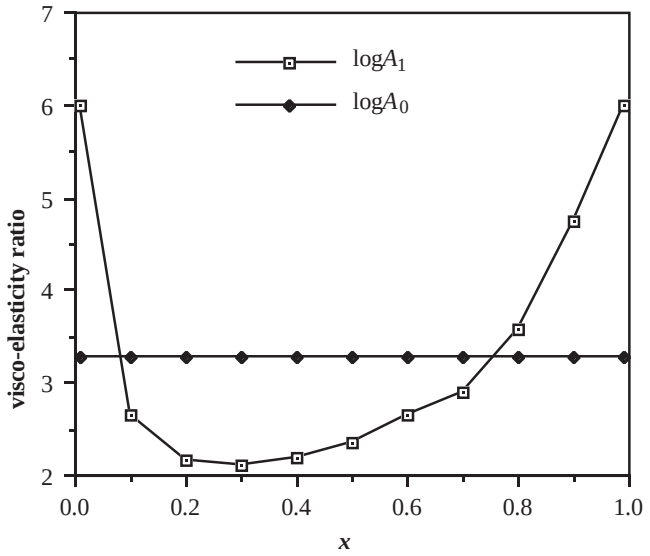

Figure 7. The visco-elasticity ratio A_1 calculated from the estimated parameters plotted against distance along the body. For explanation see text.

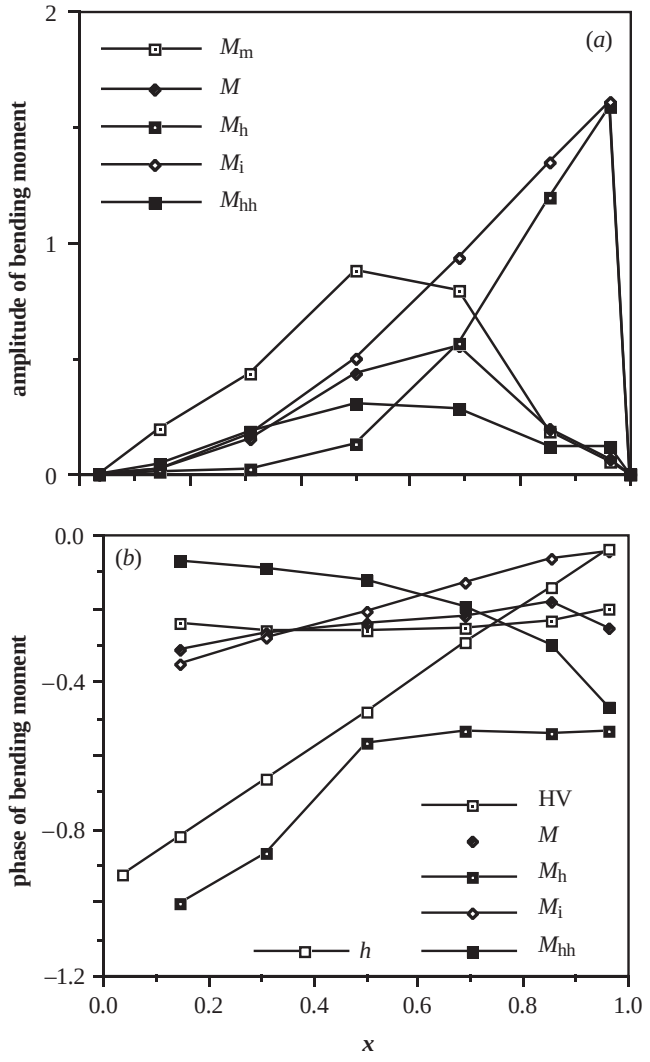

Figure 8. (*a*) The amplitude and (*b*) the phase distributions of bending moment along the body length. HV: results of the elongated-body theory (Hess & Videler 1984). M_h: fluid reaction; M_i: body inertia; M: fluid reaction and body inertia; M_{hh}: fluid reaction recoil corrected for a massless fish; M_m: muscle; h: displacement.

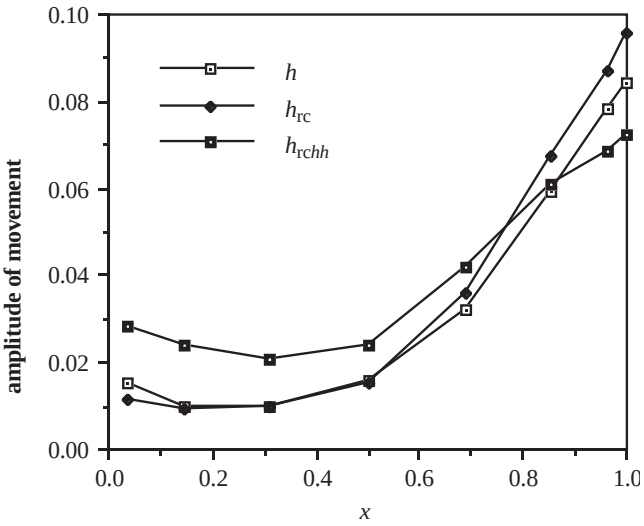

Figure 9. The amplitude distributions of the movement along the body length before (h) and after recoil correction made for a fish with (h_{rc}) and without (h_{rchh}) mass.

Table 1. *Body dimensions and kinematic data for an 'average' saithe*

total body length	$l_B = 0.40$ m
height of tail fin at trailing edge	$b_t = 0.24\, l_B$
half span	$b = 0.12\, l_B$
body volume	$= 0.0113\, l_B^3$
wetted area	$A_e = 0.401\, l_B^2$
Reynolds number	$Re = \frac{U l_B}{V} = 2 \times 10^5 - 8 \times 10^5$
time period	$T_t = 0.278$ s
swimming speed	$U = 0.86 \frac{l_B}{T_t} (U' = 0.86)$
amplitude at the tail end	$h_m = 0.083 l_B$
wave speed of undulation (whole body)	$V = 0.98 \frac{l_B}{T_t}$
wave speed of undulation (posterior half)	$V = 1.04 \frac{l_B}{T_t} (V' = 0.98)$
ratio of swimming speed to wave speed (whole body)	$\frac{U}{V} = 0.878$
reduced frequency	$\gamma = \frac{2\pi}{U'} = 7.30$
wave number	$k = \frac{2\pi}{V} = 6.41$

approximate. As a first step in modelling we will not subdivide the three regions further but assume some average properties for each.

(a) *Region 1*

Hebrank has studied the mechanical properties of Norfolk spot and skipjack tuna (Hebrank 1982). Because the spot can be described as a subcarangiform swimmer, the measured data for it may not be far from those for the saithe. Data from lateral bending tests on the backbone might have been acceptable for our model, but unfortunately they are incomplete and cannot be used. Tension tests on vertebrae with intervertebral joints give an exponential stress–strain regression

$$\ln \sigma = 0.86\epsilon + 9.82, \qquad (45)$$

Downloaded from http://rstb.royalsocietypublishing.org/ on January 16, 2018

where stress is in $\mathrm{N\,m^{-2}}$. Unlike that of the skipjack tuna the backbone of the spot shows uniform stiffness along its length, and is more flexible than in the skipjack tuna.

From (8) the maximum strain in the body is

$$\epsilon_{\max} = \left(\frac{z}{R}\right)_{\max} = -z_{\max}\left(\frac{\partial^2 h}{\partial x^2}\right)_{\max}. \tag{46}$$

For swimming saithe the maximum curvature occurs near the tail (Videler & Hess 1984) and

$$\left(\frac{\partial^2 h}{\partial x^2}\right)_{\max} \approx 4.0, \tag{47}$$

i.e. $4/l_{\mathrm{B}}$ in dimensional terms. The radius of the backbone, $z_{\max}$, is about one-fifth of the body half-thickness in the middle, so we have

$$z_{\max} = \frac{1}{5}a_{3\mathrm{m}} = \frac{1}{5}0.021 = 0.0042. \tag{48}$$

Thus, the maximum strain of the saithe backbone might be about

$$|\epsilon_{\max}| = 0.0168 \approx 2\%. \tag{49}$$

At this value of strain, equation (45) gives the stress σ to be approximately $22\,\mathrm{kN\,m^{-2}}$. From figure 4 in Hebrank's paper, the $\sigma - \epsilon$ curve can be viewed as linear for $\epsilon < 3\%$, and gives the following estimate of Young's modulus:

$$E = \frac{\sigma}{\epsilon_{\max}} = 1.1\,\mathrm{MN\,m^{-2}}. \tag{50}$$

Bennet *et al.* (1987) also measured the mechanical properties of the backbone in a cetacean (*Phocaena*) to examine the influence of elastic mechanisms in the cetacean tail on the energy cost of swimming: the question has been re-examined by Blickhan & Cheng (1994). Compression tests done on specimens consisting of two half-centra with the intervening intervertebral disc showed that the stiffness is slightly variable along the vertebral column. The maximum value of stiffness from their work is approximately

$$E = 13\,\mathrm{MN\,m^{-2}}. \tag{51}$$

Thus, the Young's modulus of backbone in carangiform fish may be taken as about 1.1–13 $\mathrm{MN\,m^{-2}}$. In non-dimensional form this gives

$$E_1 = 5 \times 10^2 - 6 \times 10^3. \tag{52}$$

Although Hebrank's study shows that the loading response curves of backbone also exhibit some hysteresis, the viscosity of backbone is considered to be unimportant compared with that of other regions and is neglected here:

$$\mu_1 = 0. \tag{53}$$

(b) *Region 2*

We have found no data for the passive mechanical properties of fish muscle. The Young's modulus for human striated skeletal muscle has been estimated to be between $1\,\mathrm{MN\,m^{-2}}$ (for muscle fibres) and $100\,\mathrm{MN\,m^{-2}}$ (for pure collagen), and for myofilaments, calculated from statistical theory, to be $1\,\mathrm{kN\,m^{-2}}$ (Schneck 1992). In fact, region 2 is composed of myomeres, myosepta and other connective tissue, and in the middle section of the body there are other units such as viscera, heart, and other parts of the circulatory and digestive systems. Assuming that this part is significantly less stiff than backbone, an average passive Young's modulus for region 2 of around $10^5\,\mathrm{N\,m^{-2}}$ is taken, giving a non-dimensional value

$$E_2 = 50. \tag{54}$$

The viscosity of striated skeletal muscle *in vivo* is between *ca.* 10^6 and 10^8 poise, and for isolated muscle is between *ca.* 10^4 and 10^5 poise at 37 °C (Schneck 1992). The body temperature of the saithe rarely exceeds 15 °C (all experiments on saithe muscle have been done at 12 °C). The passive viscosity of fish muscle will probably be no larger than that for human isolated muscle. Also the elements other than muscle would have less damping ability. We assume a viscosity for region 2 of 10^4–10^5 poise, or in non-dimensional form

$$\mu_2 = 1.7\text{–}17. \tag{55}$$

(c) *Region 3*

The fish skin gives protection from the environment and its special surface properties may help to reduce hydrodynamic drag. It may also act as an external tendon to transmit the force of muscle contraction down the length of the fish (Hebrank 1980; Wainwright 1983). However, recent measurements suggest that the role of skin is not important in body bending (J. L. van Leeuwen, personal communication). The tensile elastic modulus for eel skin is 14.6 $\mathrm{MN\,m^{-2}}$ in circumferential and 3.5 $\mathrm{MN\,m^{-2}}$ in longitudinal directions, both measured on the steep part of the J-shaped stress–strain curve (the horizontal part corresponds to a process of change in fibre angle). For shark, the longitudinal stiffness is 0.8–3.0 $\mathrm{MN\,m^{-2}}$ and may be controlled by internal pressure (Wainwright 1983). We therefore assume that the Young's modulus for saithe skin is of the order of $3.5\,\mathrm{MN\,m^{-2}}$, or in non-dimensional form

$$E_3 = 1.7 \times 10^2. \tag{56}$$

The viscosity of skin was studied in eel (Hebrank 1980), but not quantified. Here, we assume the skin viscosity coefficient to be of the same order of magnitude as that of muscle, i.e.

$$\mu_3 = 1.7\text{–}17. \tag{57}$$

7. PASSIVE VISCO-ELASTICITY EFFECTS

(a) *Free oscillation of the fish body segment in air*

An assessment of whether the above estimates of passive mechanical properties are reasonable can be made if we consider the motion of an inert segment of the body in air, as done for the lamprey by Bowtell & Williams (1991). For example, we could take a dead fish by the head, displace the caudal end sideways and then release it. Common observation suggests that the fish would return to the straight condition without oscillating; that is the body or body segment should be overdamped. This would be yet more true for a shorter segment. It is instructive to see whether the present model predicts that.

Downloaded from http://rstb.royalsocietypublishing.org/ on January 16, 2018

The response of the model is governed by equation (31) without either the muscle force term M_m or the hydrodynamic force M_h, i.e.

$$\frac{\partial^2}{\partial x^2}\left[\overline{E}I\frac{\partial^2 h}{\partial x^2}\right]+\frac{\partial^2}{\partial x^2}\left[\overline{\mu}I\frac{\partial}{\partial t}\frac{\partial^2 h}{\partial x^2}\right]+m_b(x)\frac{\partial^2 h}{\partial t^2}=0. \tag{58}$$

For a short segment, the coefficients $\overline{E}I$, $\overline{\mu}I$ and m_b may be taken as constant, so we have

$$\overline{E}I\frac{\partial^4 h}{\partial x^4}+\overline{\mu}I\frac{\partial}{\partial t}\frac{\partial^4 h}{\partial x^4}+m_b\frac{\partial^2 h}{\partial t^2}=0. \tag{59}$$

Employing the method of superposition of normal modes, we take

$$h(x,t)=\psi(x)\,e^{i\omega t}. \tag{60}$$

Substituting into (59) yields

$$-\frac{d^4\psi}{dx^4}-\beta^4\psi=0, \tag{61}$$

where

$$\beta^4=\frac{m_b}{\overline{E}I+i\omega\overline{\mu}I}\omega^2, \tag{62}$$

and $\psi(x)$ is a function of the coordinate x, defining the shape of the normal modes of oscillation. The general solution of (61) can be expressed as

$$\psi(x)=C_1\sin\beta x+C_2\cos\beta x+C_3\sinh\beta x+C_4\cosh\beta x, \tag{63}$$

in which $C_1\ldots C_4$ are constants which can be determined in each particular case from the boundary conditions of the problem. There are three types of end conditions commonly used in beam theory: (1) hinged end, $\psi=\psi''=0$; (2) fixed end, $\psi=\psi'=0$; (3) free end, $\psi''=\psi'''=0$; where a prime denotes differentiation d/dx. Here, we take the segment as a cantilever beam with one end fixed (at $x=0$) and the other end free ($x=\Delta l$). The boundary conditions for ψ are

$$\psi(0)=\psi'(0)=\psi''(\Delta l)=\psi'''(\Delta l)=0. \tag{64}$$

By setting the characteristic determinant equal to zero,

$$\begin{vmatrix}\sin\beta\Delta l+\sinh\beta\Delta l & \cos\beta\Delta l+\cosh\beta\Delta l\\ \cos\beta\Delta l+\cosh\beta\Delta l & \sinh\beta\Delta l-\sin\beta\Delta l\end{vmatrix}=0, \tag{65}$$

we obtain the frequency equation for the body segment

$$\cos\beta\Delta l\cosh\beta\Delta l=-1. \tag{66}$$

The first five roots, for example, are

$$\beta_n\Delta l=1.875,4.694,7.855,10.996,14.137. \tag{67}$$

From (62), we therefore have

$$m_b\omega_n^2-i\overline{\mu}I\beta_n^4\omega_n-\overline{E}I\beta_n^4=0, \tag{67}$$

so the eigenvalues or complex 'natural frequencies' are

$$\omega_n=\frac{i\overline{\mu}I\beta_n^4\pm i(\beta_n)^2((\overline{\mu}I)^2(\beta_n)^4-4m_b\overline{E}I)^{1/2}}{2m_b}. \tag{69}$$

If the system is indeed overdamped, the 'natural frequencies' can be written as

$$\omega_n=i\phi_n, \tag{70}$$

where the ϕ_n are real and positive. From (69) this requires that

$$\frac{4m_b\overline{E}I}{(\overline{\mu}I)^2}\leqslant\beta_n^4. \tag{71}$$

Since $\beta_1\Delta l$ is the first root of the characteristic equation, i.e. the one with smallest magnitude, it is sufficient to have

$$\frac{m_b\overline{E}I}{(\overline{\mu}I)^2}\leqslant\frac{1}{4}\left(\frac{1.875}{\Delta l}\right)^4. \tag{72}$$

To see whether the above parameter estimates are reasonable, we substitute them into the inequality (72). We note first that, if the cross-section of the fish body has essentially the same shape from the head to just before the tail, varying only in scale, then the left-hand side of (72) is inversely proportional to the square of a typical dimensionless width, say a_3^{-2}. Also, the right-hand side is inversely proportional to the fourth power of the segment length. Thus, the inequality is most likely to be satisfied for wider, shorter segments. The main result is clearly that, other things being equal, the tissue viscosity must be large enough for the inequality to be satisfied.

From the estimates here, and the data of Hess & Videler (1984), we first take data roughly according to the widest section (recall that lengths are made dimensionless with respect to body length): $m_b=0.03$, $b_3=0.12$, $a_3=0.06$, $a_1=0.01$, $\Delta h=0.02a_3$, (refer to equations (19) and (20)). We also take $E_1=10^3$ (equation (52)), $E_2=50$ (equation (54)), $E_3=1.7\times10^2$ (equation (56)), and $\mu_2=\mu_3=17$, the highest value from equations (55) and (57). Then

$$\overline{E}I=1.2\times10^{-3},\ \overline{\mu}I=3.4\times10^{-4},$$

and inequality (72) is satisfied only if $\Delta l<0.38$: i.e. the segment length should be less than 28% of body length. That is rather small, suggesting that long segments of fish may not be overdamped, but great accuracy is not to be expected because the fish is not uniform along its length (as assumed) and the estimates for E and μ are very rough. In particular, an even larger value for tissue viscosity would reduce the tendency to oscillation: if $\overline{\mu}$ is multiplied by 4, the value of Δl needed to satisfy (72) is multiplied by 2.

(b) *Distribution of passive effects along the body*

We now examine more closely the distribution of passive effects along the fish body. The bending modulus depends not simply on the viscous and elastic coefficients of the materials in the body, but also on the dimensions and shape of the cross-sections. The logarithms of the second moments of the three regions and the first area moment of half of region 2 are plotted against the body length in figure 5 based on the data of Hess & Videler (1984). Excluding the head and peduncle, the second area moment of region 2, i.e. I_2, is respectively three and two orders of magnitude higher than that of regions 1 and 3, i.e. I_1 and I_3. This means that for the part of the body in $0.2\leqslant x\leqslant0.8$, and if the three regions consisted of the same materials, the bending behaviour of the whole body would be dominated by region 2. However, the contribution of region 3 (skin) is at least one order of magnitude higher than that of region 1 (backbone).

Downloaded from http://rstb.royalsocietypublishing.org/ on January 16, 2018

Table 2. *Viscous and elastic coefficients used in calculations*

	E	μ
region 1	10^3	0
region 2	10	10
region 3	10^2	10

From the estimates in § 6, and the conclusions of § 7a, we take characteristic values of the viscous and elastic coefficients of the three regions to be as shown in table 2, and these will be used in subsequent calculations. In general, the values of the elastic moduli are considered to be close to reality in regions 1 and 3, but have considerable uncertainty in region 2, probably the most important. These values cannot be regarded as an accurate description of the mechanical properties of a fish body and are used only to give an indication of the influence of body tissues during bending in the calculated examples. Indications of what would happen for larger or smaller values of the moduli are also presented.

Denoting the ratio of elastic and viscous bending moduli of each region to that of the whole cross-section respectively as

$$r_{\mathrm{em}i} = \frac{E_i I_i}{\overline{E}I}, \; r_{\mathrm{vm}i} = \frac{\mu_i I_i}{\overline{\mu}I}, \; i = 1,2,3, \tag{73}$$

and taking the values in table 2, we plot the ratios of elastic and viscous bending moduli against distance down the body in figure 6. For $0.2 \leqslant x \leqslant 0.7$, $r_{\mathrm{em2}} > 50\%$, and $20\% < r_{\mathrm{em3}} \leqslant 30\%$ approximately. So in resisting local elastic-bending region 2 provides the largest contribution with a significant supplement from the skin, although region 2 is much more compliant than either skin or backbone; r_{em2} decreases and r_{eml} increases towards the tail. At around $x = 0.7$, just before the caudal peduncle, the three ratios of the elastic bending moduli are comparable. At the peduncle, $0.75 \leqslant x \leqslant 0.9$, the elastic bending modulus is dominated by the contribution from the backbone. As we have used the same viscous coefficients for regions 2 and 3, the viscous bending modulus is almost totally determined by the contribution from region 2.

The combined dynamic behaviour of the passive viscous and elastic materials of the body is reflected by the complex fundamental frequency (69), as discussed in §7a. If we take a segment of length $\Delta l = 0.2 l_{\mathrm{B}}$, then the right-hand side of (72) takes the value $A_0 = 1900$. Corresponding values of the left-hand side (A_1) at different sites along the body are plotted in figure 7. They show, as expected, that overdamping should occur on the trunk, but not necessarily on the peduncle and tail.

In principle, the general motion of the fish in water may be obtained by solving equation (29) when the active muscle bending moment is given; the general inhomogeneous problem can be solved as soon as the homogeneous equation has been solved to give the normal modes of free oscillation, because the motion can be represented by a superposition of normal modes. However, there are difficulties in following this approach. For example, because the coefficients in the equation, such as $\overline{\mu}I$ and $\overline{E}I$, are not constants for the whole fish, we cannot calculate the normal modes analytically. Furthermore, the hydrodynamic force cannot be written as an explicit formula. For a slender eel-like fish with an approximately uniform body, it may be possible to derive the motion analytically for a given distribution of muscle bending moment, with the hydrodynamic force calculated from the elongated-body theory. In general however, and in particular for the saithe, it is not possible. That is why we take the other approach here: start with the measured displacement wave, and infer M_{m} from equation (29).

8. RESULTS AND DISCUSSION

(a) *Bending moment distribution*

In the present linear model, the bending moment required from muscle contraction, i.e. the active muscle bending moment, is determined by a simple sum of three contributions: fluid reaction, body inertia and internal tissue, as described by equation (31), i.e.

$$M_{\mathrm{m}} = -(M_{\mathrm{e}} + M_{\mathrm{v}} + M_{\mathrm{h}} + M_{\mathrm{i}}) = -M_{\mathrm{p}} + M. \tag{74}$$

The net bending moment M is balanced by the fluid reaction and body inertia ($M_{\mathrm{h}}+M_{\mathrm{i}}$), which have previously been calculated by using the same hydrodynamic method and kinematic data (Cheng & Blickhan 1994). Each term in (74) may be further explained as follows.

1. M_{h}: the hydrodynamic bending moment. This term represents the bending moment required by a flexible body, with no mass or influence of passive internal biomaterials, swimming in water, performing the measured undulation pattern and with recoil correction calculated for a real saithe.
2. M_{i}: the inertial bending moment. This may be viewed as being required when a flexible body, without the influence of passive internal materials, 'swims' in air with the same body movement as in water.
3. M_{e}, M_{v} and M_{p}: the elastic, viscous and total passive bending moments. These would be equivalent to those required by a flexible body without mass moving in air.

We will discuss each individual contribution and their mutual operation. The calculation of each bending moment is made by using the same movement pattern, recoil corrected with respect to the measured pattern. Note that such a movement already reflects the influence of body inertia as well as the hydrodynamics.

(i) *Individual contributions, M_{h}, M_{i} and M*

Figure 8*a*,*b* gives the amplitude and phase distribution of M_{h} and M_{i} along the body, respectively. It can be seen from figure 8*a* that the amplitude of M_{h}, i.e. M_{hl}, is lower than that of M_{i} along most of the body, and that both increase from zero at the head, approach each other towards the tail, and fall to zero at the tail tip. It is interesting to note that the amplitude of M is lower than that of M_{i} along the whole body and much lower than both M_{il} and M_{hl} when $x > 0.7$. M_{h} and M_{i} are not simply added to determine the moment required from muscle contraction. In fact, from figure 8*b* M_{i} and M_{h} are almost 180° out of phase on the caudal part of the body. This means that the required inertial bending moment is supplied by the fluid reaction. The unsteady flow produced by body bending

Downloaded from http://rstb.royalsocietypublishing.org/ on January 16, 2018

Table 3. *The average speeds of the bending moment waves along the body length, measured in body lengths per tail-beat period*

(EMG-onset data: saithe, Wardle & Videler (1993); carp, van Leeuwen *et al.* (1990).)

	speed between $0.31 \leqslant x \leqslant 0.5$	speed between $0.5 \leqslant x \leqslant 0.85$
h	1.01	1.14
h_{xx}, M_e, M_v	1.31	0.91
M_h	0.64	13.83
M_{hh}	−5.55	−2.04
M_i	2.71	2.46
M	8.42	5.86
M_p	1.29	0.73
M_m	1.32	2.19
M_m	1.54 ($0.31 \leqslant x \leqslant 0.69$)	—
EMG-onset (saithe)	1.5−1.6 ($0.4 \leqslant x \leqslant 0.65$)	—
EMG-onset (carp)	1.6	—

not only promotes swimming propulsion but at the same time can provide considerable bending moment to move the body with its particular mass distribution. The model therefore suggests that a swimming fish uses the fluid reaction to balance the change of local lateral momentum of its body. In this way M, i.e. the bending moment required to balance the combined fluid reaction and body inertia, is largely reduced and muscle energy may be saved. Note that these conclusions are independent of the choice of passive mechanical properties of the fish tissues.

From figure 8*b* we find that the phase of M_h is almost constant over the rear-half of the body. This means that to undulate the body in water a standing wave of side-to-side force on that part is needed to balance the fluid reaction. Hess & Videler (1984) suggested that a standing wave of bending moment may be required to balance the combined fluid reaction and body inertia. However, later studies (Cheng *et al.* 1993; Cheng & Blickhan 1994) suggested that such a bending moment still behaves as a travelling wave although its speed is much greater than that of body bending. This is seen in figure 8*b*, which also shows that the inertial bending moment travels faster than body curvature and more slowly than the hydrodynamic bending moment. The wave speeds of the bending moments due to each mechanism, averaged over $0.31 \leqslant x \leqslant 0.5$ and $0.5 \leqslant x \leqslant 0.85$ from the present calculations, are given in table 3.

If we consider a massless saithe-like 'fish', i.e. assume $m_b(x) = 0$ and use the measured movement of the saithe as input, the recoil-corrected bending moment, M_{hh}, is also as shown in figure 8. The displacement amplitudes along the body before and after recoil correction are given in figure 9. Of course this case does not exist in reality, but is used to show other theoretically possible forms of the hydrodynamic bending moment distribution. The massless 'fish' achieves a larger recoil than a real saithe and the variation of the amplitude of undulation is smaller (figure 9). However, the required bending moment behaves as a forward travelling wave, i.e. the wave of muscle contraction should start at the tail and move gradually

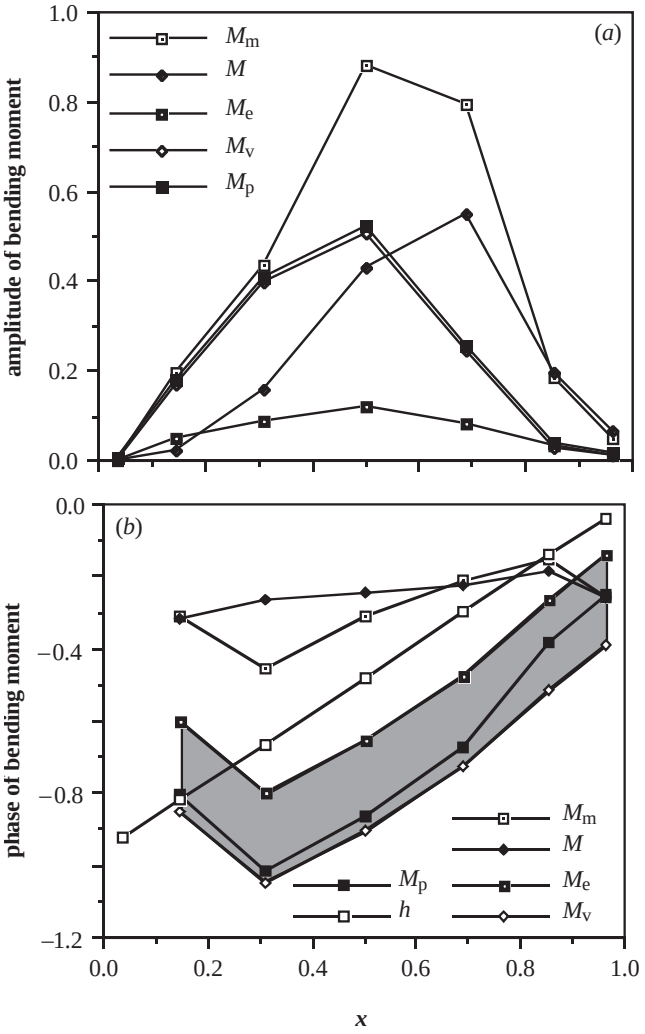

Figure 10. (*a*) The amplitude and (*b*) phase distributions of bending moment along the body. M_e: elasticity; M_v: viscosity; M_p: total passive mechanical properties; M: both fluid reaction and body inertia; M_m: muscle activation required by the mutual operation of all factors.

forward (figure 8*b*). This finding emphasises how external hydrodynamic processes can significantly influence the internal dynamics.

(ii) *Individual contributions, M_e, M_v and M_p*

The bending moment distribution due to elasticity, viscosity and total passive properties within the body, i.e. M_e, M_v and M_p, are given in figure 10*a*,*b*, where they can be compared to the distribution of M (note that the scale of figure 10*a* is different from that of figure 8*a*). The amplitude of M_p is very close to that of M_v, and both are larger than M_e except in the peduncle region, as required by the overdamping condition. The amplitudes of M_e, M_v and M_p are close to each other on the narrow neck of the peduncle and the tail, where the viscous bending moment, dominated by the contribution from region 2, is reduced and the elastic backbone (region 1) becomes important (figures 5, 6 and 7).

The greatest uncertainty in our estimates of the passive mechanical properties lay in the value of E_2, which dominates $\overline{E}$ over the central part of the fish body.

Downloaded from http://rstb.royalsocietypublishing.org/ on January 16, 2018

However the results of figure 8*a* show that even if its value were five times larger the amplitude of M_e (proportional to $\overline{E}$) would still only be comparable with M_v (given our estimated μ_2) and the maximum of M_p would increase by a factor of about $\sqrt{2}$. The last result follows from writing M_e, M_v and M_p in a form similar to (37), and from (40) the amplitude M_p is

$$M_{p1}(x) = (\overline{E}I^2 + (2\pi\overline{\mu}I)^2)^{1/2} h_{xx1}(x) = (M_{e1}^2 + M_{v1}^2)^{1/2}. \tag{75}$$

Thus, figure 10*a* would not be greatly affected by such an underestimate. It would be even less affected if E_2 were an overestimate, because M_e would become negligible. An increase in the value of μ_2 would have a proportianally greater effect, because M_v is estimated to be larger than M_e.

However, no changes in the absolute values of the passive mechanical moduli will have much effect on the phases of the M_e, M_v, and M_p waves (figure 10*b*), at least as long as the relative distribution of the different materials remain mostly unaltered. From figure 10*b*, we see that the wave speeds of the elastic and viscous bending moments and the bending curvature (not shown) are the same. From (26), (27) and (40), the phase functions of the bending moments M_e, M_v and M_p can be determined as

$$\tau_{Me}(x) = \tau_{hxx}(x) - \frac{1}{2}, \tag{76a}$$

$$\tau_{M_v}(x) = \left(t_{hxx}(x) - \frac{1}{2}\right) - \frac{1}{4}, \tag{76b}$$

$$\tau_{M_p}(x) = \left(\tau_{hxx}(x) - \frac{1}{2}\right) - \frac{1}{2\pi} tg^{-1}\left(\frac{2\pi\overline{\mu}I}{\overline{E}I}\right), \tag{76c}$$

where $\tau_{hxx}(x)$ is given by (34). There is a constant phase difference, i.e. a quarter of one period, between M_e and M_v. Because $\overline{\mu}I$ and $\overline{E}I$ are not negative, we have

$$0 \leqslant tg^{-1}\left(\frac{2\pi\overline{\mu}I}{\overline{E}I}\right) \leqslant \frac{1}{4}. \tag{77}$$

This means that under the present linear assumption, no matter what magnitudes the mechanical moduli of the biomaterials in the fish may have, the phase of their bending moment wave must be within the range bounded by those of M_e and M_v, i.e. the hatched area shown in figure 10*b*. From the figure we can see that the wave speed of M_p may be a little lower or higher than that of the bending curvature, but cannot be higher than that of M. The wave speeds calculated by using the present parameters are also given in table 3.

(iii) *Muscle contribution* M_m

When all the relevant factors are combined—hydrodynamic, inertial and passive mechanical—we can finally estimate the bending moment generated by the muscle itself, M_m. This has been given in both figure 8 and figure 10. The amplitude of M_m is higher than both M_p and M along most of the fish's length before the narrow peduncle. Its peak position ($x \approx 0.6$) is located behind the mid-point and between that of M_p ($x \approx 0.45$) and M($x \approx 0.65$). Thus, the maximum bending moment is predicted to be produced by the muscle at $x \approx 0.6$. The phase of M_m is between that of M_p and M on the middle part of the body. The wave speed of M_m (see table 3 and figure 10*b*) is lower than that of M and higher than that of M_p. Of course, if the passive elastic moduli were larger, then M_m would tend more to M_p; if smaller, it would tend more to M.

The behaviour of the muscle bending moment is considered to correspond to that of muscle activation. EMG studies show that muscle activation is strictly left–right alternating. Therefore, it is appropriate that the muscle bending moment be described by a wave function with a time-averaged value of zero, as contraction is defined as positive on one side and negative on the other (figure 3).

The activation of the muscle in saithe has been found experimentally to behave like a travelling wave, with an average speed (EMG-onset) of 1.4–1.6 body lengths per period of undulation for $0.4 \leqslant x \leqslant 0.65$ (Wardle & Videler 1993), which is faster than the wave speed of undulation: about one body length per period. A similar result can be estimated from the measurements on carp (van Leeuwen *et al*. 1990) to give a speed of 1.6 lengths per period. Rather surprisingly, given the uncertainties of the model, the predicted average wave speed of the muscle bending moment M_m for $0.31 \leqslant x \leqslant 0.69$ (see table 3), covering the range of body lengths studied in EMG measurements, is 1.54 body lengths per period, which is almost the same as that obtained from the EMG.

(b) *Activation pattern of the contractile element*

As seen here, the time course of M_m corresponds to the time-course of muscle contraction derived from EMG experiments. The onset and end of EMG activity in the left side of a swimming saithe (or mackerel) at two positions $x = 0.4$ and 0.65, and the time-course of the maximum muscle bending moments along the body length calculated by the present model, are shown in figure 11. Zero and one on the vertical time axis correspond to the instant before the tail tip shows any motion in the right-going tail sweep. The duration of EMG activity decreases along the body; the duration of the muscle bending moment remains constant everywhere (half the tailbeat period) and is shown by the shaded area in figure 11, within which any phase curve represents the propagation of a fixed oscillating phase.

As the wave speed of M_m is very close to that of EMG-onset, the phase curve of M_m-onset, i.e. the wave front of M_m, maintains an almost constant phase difference (about 12% T_l) from the EMG-onset. This is related to the observed time delay between the EMG signal and the peak force (or bending moment) generation owing to the mechanical and contractile properties of muscle: 25–45 ms in the saithe (Altringham *et al*. 1993). As the measured period is $T_l = 0.278$ s, for saithe, this additional delay is of the order of 10% of a cycle. The theoretically predicted time-course of the onset of the muscle bending moment is therefore quite close to that of muscle force generation. It follows that, in steady swimming, the observed muscle activation pattern closely matches the dynamic response of the entire system of the body and water as calculated here.

Figure 11 shows that the duration of EMG activity decreases towards the rear of the fish, and is always shorter than the duration of the muscle bending moment, which is constant at half of one tailbeat cycle. The

Downloaded from http://rstb.royalsocietypublishing.org/ on January 16, 2018

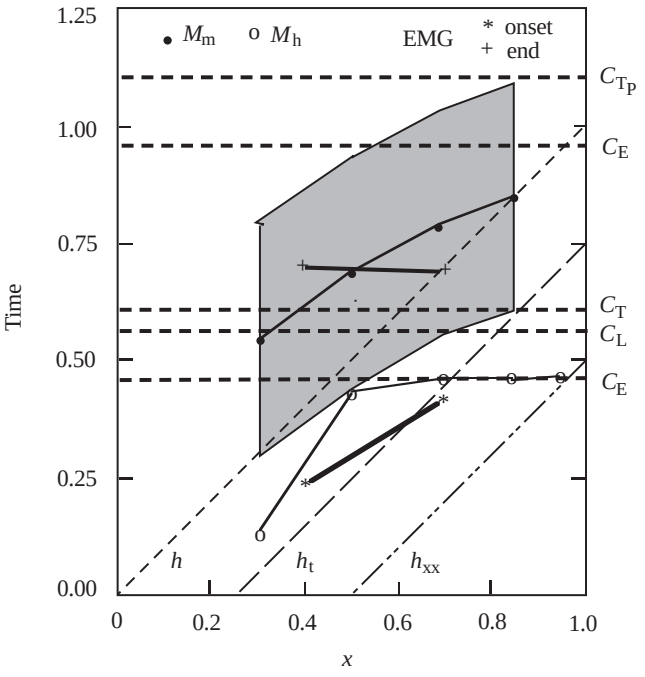

Figure 11. The time-courses of the onset and end of EMG activity on the left side of a swimming mackerel or saithe (Wardle & Videler 1993), and of the muscle bending moment (M_m) along the body length calculated by the present theory for saithe. Values 0 and 1 on the time axis correspond to the times of leftmost tail-tip position which are defined as the time origin. The shaded area represents the duration of the bending moment produced by muscle activation on the left side. M_m, M_h, h_t, h_{xx}, C_{Tp}, C_E, C_L: the phase of maximal muscle bending moment, hydrodynamic bending moment, lateral velocity, curvature (muscle at minimum length on left side), total thrust, hydrodynamic power, left-pointed lateral force.

maximum bending moment occurs within the EMG period anteriorly, but after it posteriorly.

Why the end of the EMG signal is different from the calculated end of the M_m wave is not clear at present. The constant duration of the bending moments along the body length is a direct outcome of the linear model used here. Nonlinearity in the mechanical properties of the internal tissues and in the hydrodynamic force may make the hydrodynamic and passive bending moments have a different duration or time-dependence relative to body bending. In this way the behaviour of M_m could be changed. The linear assumption holds for small amplitude undulations and is generally not far away from the real situation for steady carangiform swimming in fish such as saithe. Perhaps a more important effect is nonlinearity of the contractile and mechanical properties of active muscle. It is thus important to examine whether the active phase of muscle contraction, i.e. the measured duration of the EMG activity, can produce a force duration close to the observed half-period of body undulation. This has indeed been observed by Altringham *et al.* (1993) who also showed that the active properties of the muscle vary along the body length (see next section for further discussion).

As discussed in § 8a,ii, the wave speed of M_p is close to that of curvature. So during bending, the dynamic response of the passive internal tissues has only a small phase difference with respect to the local strain along the body. M_i and particularly M_h have much higher wave speed than body curvature, and both have a variable phase difference with the local strain. As the result of interaction among the dynamic processes of the internal tissues, and fluid and body inertia, a wave of muscle bending moment is needed, from the muscle activation, with a speed greater than that of body bending. Thus, a faster wave of muscle activation with a variable phase relation between the strain and activation cycle along the body, as observed in EMG studies (Williams *et al.* 1989; van Leeuwen *et al.* 1990; Wardle & Videler 1993), is found from the present study to be required by the fluid dynamic mechanism and, to a lesser extent, the body inertia force.

(c) *Body bending and hydrodynamic propulsion*

Many studies on the pattern of muscle contraction in fish have been related to the hydrodynamic propulsion generated by the body and tail (Hess & Videler 1984; Williams *et al.* 1989; van Leeuwen *et al.* 1990; Wardle & Videler 1993; Altringham *et al.* 1993). Based on the point of view that the lateral hydrodynamic force acting on the caudal fin might be in phase with the lateral velocity (Lighthill 1977), efforts were made to relate the timing of muscle activity to maximal thrust by the caudal fin in carangiform fish.

First, the hydrodynamic lateral force on a fin is known to have a phase delay behind the lateral velocity of the fin because of shedding of vortices at the trailing edge. Lighthill suggested that the 'Wagner effect', i.e. the phase delay, may vanish when the reduced frequency of a 2D rigid oscillating plate reaches a value close to 0.7 (Lighthill 1977). However, we know that the Theodorsen function determining the phase of the lateral force is very sensitive to frequency at low values. Furthermore, the tail of a carangiform fish is not rigid. From the kinematic data for saithe and other fishes, there can be a phase difference of up to one tenth of the undulation cycle in the lateral velocity itself between the leading and trailing edges of the tail. So the lateral hydrodynamic force acting on the tail is not necessarily in phase with the lateral velocity of the tail tip (trailing edge).

Second, the lateral force is not equivalent to the thrust, which is the component of the force in the swimming direction. The thrust is determined by the distribution of the lateral force multiplied by the local angle of attack on the tail. In general, the maximal thrust also does not occur at the instant of maximal lateral force.

According to the 3D flexible plate model of fish swimming (Cheng *et al.* 1991), the total thrust due to pressure differences on the plate, the hydrodynamic power to maintain the movement of the plate in water, and the lateral force can be derived, and their coefficients can be written as

$$\begin{aligned} C_{T_p} &= C_{T_{p0}} + C_{T_{p1}}\cos 2\omega t + C_{T_{p2}}\sin 2\omega t \\ &= C_{T_{p0}} + C_{T_{p3}}\cos 2\omega t(t - \tau_{CT_p}) \\ C_E &= C_{E0} + C_{E1}\cos 2\omega t + C_{E2}\sin 2\omega t \\ &= C_{E0} + C_{E3}\cos 2\omega(t - \tau_{CE}) \\ C_L &= Re(\tilde{C}_L e^{i\omega t}) = C_{L1}\cos\omega(t - \tau_{CL}). \end{aligned} \tag{78}$$

Downloaded from http://rstb.royalsocietypublishing.org/ on January 16, 2018

The cycle period of thrust and power is half that of the displacement. By using the same data as in the bending moment calculation, the propulsive energetic quantities may be obtained. The phase of maximal thrust, power and lateral force: τ_{CTp}, τ_{CE}, τ_{CL} are also shown in figure 11.

From the present results we can see that the thrust produced by the whole body undulation, but mostly by the tail, lags the lateral force a little, and is close in phase to the lateral velocity not at the tail tip but in the peduncle region in agreement with Altringham *et al.* (1993): see their figure 8, where the caudal peduncle crosses the swimming track as peak muscle power is generated. The maximal thrust and lateral force occur at the instant of maximal muscle bending moment anterior to the middle point of the body, and both occur before the muscle is switched off. The hydrodynamic bending moment at the rear is almost in phase with the hydrodynamic power required to maintain undulation of the plate in water.

Only in the anterior part of the body does force development by muscle activation coincide with propulsive force generation at the tail. Thus it may be suggested that the pattern of muscle activation within the body is not the same as that of thrust development but is determined by the operation of the whole system. A wave of muscle activation travelling faster than that of body bending is enforced by the hydrodynamic reaction, and limited by the passive internal tissues.

(d) *Stress distribution*

The longitudinal distribution of maximal passive stress at the outer boundary of each region of the cross-section can be calculated by equation (22), and the result is shown in figure 12. Only the stress amplitudes are given, as the phases are similar to those of passive bending moment. The passive stress in the backbone is much higher than in the other two regions although it experiences smaller strain. At any instant, muscle contracts only on one side of the body and the backbone may serve to resist deformation to form a neutral surface in realizing body bending, with the strain being anti-symmetric to that surface on any cross-section. With the support of the backbone the local bending is resisted mostly by region 2 (see § 7b). The backbone, and secondarily the skin, like a 'drive shaft', play a role in transmitting force and deformation to maintain and adjust the movement of the body and particularly the tail.

The average active muscle stress is also given in figure 12, based on equation (25). The fast muscle is assumed to be active during steady swimming as shown in table 1, and to be distributed over region 2 of the cross-section. In fact the fast muscle only occupies a part of the region 2, as discussed in § 6. Hence, the muscle stress distribution will not be as steep as that shown in the figure. It is clear from figure 12 that higher active stress is required from the rear part of the body, before the tail, where there is less muscle and high strain. In this region muscle is being stretched during the onset of force generation and this probably enables the muscle to sustain the high stress shown in figure 12 (Altringham *et al.* 1993). Altringham *et al.* (1993) suggested that those myotomes in $x \leqslant 0.65$ generate power at some phase of the tail beat after stiffening to transmit rostral power to the tail, but with increasing proximity to the tail, the muscle does less positive work, and may yield net negative work. More precise EMG data and dynamic measurements are needed on muscles from the caudal region. Theoretical modelling may also need to be improved to consider possible nonlinear effects at higher strains.

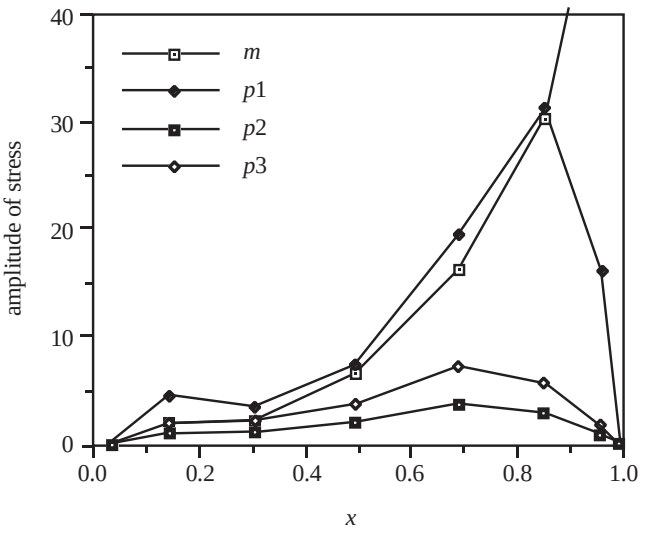

Figure 12. The amplitude distribution of stress along the body length. p_1, p_2, p_3: stress at the outer boundary of each region on the cross-section of the fish body due to passive visco-elastic properties of the internal tissues. *m*: average active muscle stress.

9. CONCLUSION

To understand how the entire locomotor system of a fish is designed to interact with the surrounding fluid to produce undulatory swimming movements, a dynamic model is presented which integrates contributions from active muscle contraction, passive internal biomaterials, body inertia and the fluid reaction. A parallel arrangement of the power unit, passive elastic unit and passive viscous unit on any longitudinal segment of the body is assumed. It is estimated that, during bending of the body, in the trunk the passive internal tissues show overdamping behaviour dominated by the myotomal muscle, and in the peduncle the elastic backbone determines local behaviour.

The body bending moment distributions corresponding to individual mechanisms and their mutual operation are analysed. The fluid reaction needs a bending moment with increasing amplitude towards the tail and near standing wave behaviour on the rear-half of the body. The inertial movement of the body results from a bending moment wave with increasing amplitude towards the tail and a higher wave speed than that of body bending. The fluid reaction, mainly designed for propulsion, also provides considerable force to balance the local momentum change of the fish body and hence to reduce the contribution required from muscle on the rear part of the body. The wave of the passive visco-elastic bending moment, with an amplitude distribution peaking a little before the mid-point of the fish, travels with a speed close to that of body bending.

The distribution of muscle bending moment, calculated from the whole dynamic system, has a wave speed almost

Downloaded from http://rstb.royalsocietypublishing.org/ on January 16, 2018

the same as that of the EMG-onset, and a starting instant close to that of muscle activation. This suggests a consistent matching between the muscle activation pattern and the dynamic response of the system in steady swimming. A wave of the muscle activation, faster than that of bending, with a variable phase relation between the strain and the activation cycle arises basically from the fluid dynamic mechanism and, to a lesser extent, the body inertia, and is limited by the passive internal tissues. In general, the active muscle force development does not coincide with propulsive force generation on the tail.

The stiff backbone may play a role in transmitting force and deformation to maintain and adjust the movement of the body and tail in the water. Higher active stress is required from caudal muscle.

The present model is limited by its basic assumptions, such as the linear and parallel arrangement of the active, elastic and viscous units within the body, the linear hydrodynamic theory and so on. More careful consideration is also needed of the caudal part of the body. Our estimates of tissue elastic moduli are very uncertain but, perhaps surprisingly, large errors in their values would have little qualitative effect on the predictions.

J.Y.C. was a postdoctoral fellow funded by a grant from the University of Leeds Academic Development Fund to support interdisciplinary research in Mathematical Biology.

REFERENCES

Alexander, R. McN. 1969 The orientation of muscle fibres in the myomeres of fishes. *J. Mar. Biol. Ass. UK* **49**, 263–290.

Altringham, J. D. & Johnston, I. A. 1990*a* Modelling muscle power output in a swimming fish. *J. Exp. Biol.* **148**, 395–402.

Altringham, J. D. & Johnston, I. A. 1990*b* Scaling effects in muscle function: power output of isolated fish muscle fibres performing oscillatory work. *J. Exp. Biol.* **151**, 453–467.

Altringham, J. D., Wardle, C. S. & Smith, C. I. 1993 Myotomal muscle function at different points in the body of a swimming fish. *J. Exp. Biol.* **182**, 191–206.

Bennet, M. B., Ker, R. F. & Alexander, R. McN. 1987 Elastic properties of structures on the tails of cetaceans (*Phocaena* and *Lagenorhynchus*) and their effect on the energy cost of swimming. *J. Zool.* **211**, 177–192.

Blickhan, R. & Cheng, J.-Y. 1993 Energy storage by elastic mechanisms in the tail of large swimmers—a re-evaluation. *J. Theor. Biol.* **168**, 315–321.

Bowtell, G. & Williams, T. L. 1991 Anguilliform body dynamics: modelling the interaction between muscle activation and body curvature. *Phil. Trans. R. Soc. Lond.* B **334**, 385–390.

Bowtell, G. & Williams, T. L. 1993 Anguilliform body dynamics: a continuous model for the interaction between muscle activation and body curvature. *J. Math. Biol.* **32**, 83–92.

Chen, Y. 1966 *Vibrations: theoretical methods*. Reading, MA: Addison-Wesley.

Cheng, J.-Y. & Blickhan, R. 1993 Bending moment distribution along swimming fish. *J. Theor. Biol.* **168**, 337–348.

Cheng, J.-Y., Zhuang, L.-X. & Tong, B.-G. 1991 Analysis of swimming three-dimensional waving plates. *J. Fluid Mech.* **232**, 341–355.

Cheng, J.-Y., Blickhan, R. & Nachtigall, W. 1993 Kinematic and dynamic properties of undulatory swimming in fish. In *Proceedings of the 2nd international conference on fluid mechanics* (ed. Qiu Shuqing), pp. 787–792. Beijing: Peking University Press.

Daniel, T., Jordan, C. & Grunbaum, D. 1992 Hydromechanics of swimming. In *Advances in comparative and environmental physiology*, vol. 11 (ed. R. McN. Alexander), pp. 17–49. Berlin: Springer.

Fung, Y. C. 1981 *Biomechanics: mechanical properties of living tissues*. New York: Springer.

Hebrank, M. R. 1980 Mechanical properties and locomotor functions of eel skin. *Biol. Bull.* **158**, 58–68.

Hebrank, M. R. 1982 Mechanical properties of fish backbone in lateral bending and in tension. *J. Biomech.* **15** (suppl. 2), 85–89.

Hess, F. & Videler, J. J. 1984 Fast continuous swimming of saithe (*Pollachius virens*): a dynamic analysis of bending moments and muscle power. *J. Exp. Biol.* **109**, 229–251.

Hill, A. V. 1938 The heat of shortening and dynamic constants of muscle. *Proc. R. Soc. Lond.* B **126**, 136–195.

Kesel, A. B., Blickhan, R. & Nachtigall, W. 1992 Patterns of muscle recruitment in different swimming modes of rainbow trout. In *Fish in ecotoxicology and ecophysiology* (ed. T. Braunbeck, W. Hanke & H. Segner), pp. 1–6. Berlin: VCH Verlag Chemie.

Karpouzian, G., Spedding, G. & Cheng, H. K. 1990 Lunate-tail swimming propulsion. 2. Performance analysis. *J. Fluid Mech.* **210**, 329–351.

Lighthill, M. J. 1960 Note on the swimming of slender fish. *J. Fluid Mech.* **9**, 305–317.

Lighthill, M. J. 1971 Large-amplitude elongated-body theory of fish locomotion. *Proc. R. Soc. Lond.* B **179**, 125–138.

Lighthill, M. J. 1975 *Mathematical biofluiddynamics*. Philadelphia, PA: SIAM.

Lighthill, M. J. 1977 Mathematical theories of fish swimming. In *Fisheries mathematics* (ed. J. H. Steele), pp. 131–144. New York: Academic Press.

Lighthill, M. J. & Blake, R. W. 1990 Biofluiddynamics of balistiform and gymnotiform locomotion. 1. *J. Fluid Mech.* **212**, 183–207.

Rome, L. C. & Sosnicki, A. A. 1991 Myofilament overlap in swimming carp. 2. Sarcomere length changes during swimming. *Am. J. Physiol.* C **260**, 289–296.

Schneck, D. J. 1992 *Mechanics of muscle*, 2nd edn. New York University Press.

van Leeuwen, J. L., Lankheet, M. J. M., Akster, H. A. & Osse, J. W. M. 1990 Function of red axial muscles of carp (*Cyprinus carpio* L.): recruitment and normalised power output during swimming in different modes. *J. Zool.* **220**, 123–145.

Videler, J. J. & Hess, F. 1984 Fast continuous swimming of two pelagic predators, saithe (*Pollachius virens*) and mackerel (*Scomber scombrus*): a kinematic analysis. *J. Exp. Biol.* **109**, 209–228.

Wainwright, S. A. 1983 To bend a fish. In *Fish biomechanics* (ed. P. W. Webb & D. Weihs), pp. 68–91. New York: Praeger.

Wainwright, S. A., Vosburgh, F. & Hebrank, J. H. 1978 Shark skin: function in locomotion. *Science* **202**, 747–749.

Wardle, C. S. 1975 Limit of fish swimming speed. *Nature* **255**, 725–727.

Wardle, C. S. & Videler, J. J. 1992 The timing of the EMG in the lateral myotomes of mackerel and saithe at different swimming speeds. *J. Fish Biol.* **42**, 347–359.

Wardle, C. S., Videler, J. J. & Altringham, J. D. 1995 Tuning in to fish swimming waves: body form, swimming mode and muscle function. *J. Exp. Biol.* **198**, 1629–1636.

Webb, P. W. & Weihs, D. 1983 *Fish biomechanics*. New York: Praeger.

Williams, T. L., Grillner, S., Smoljaninov, V. V., Wallen, P., Kashin, S. & Rossignol, S. 1989 Locomotion in lamprey and trout: the relative timing of activation and movement. *J. Exp. Biol.* **143**, 559–566.

Wu, T. Y. 1971*a* Hydrodynamics of swimming fishes and cetaceans. *Adv. Appl. Math.* **11**, 1–63.

Wu, T. Y. 1971*b* Hydrodynamics of swimming propulsion. 1. Swimming of a two-dimensional flexible plate at variable forward speeds in an inviscid fluid. *J. Fluid Mech.* **46**, 337–355.

Downloaded from http://rstb.royalsocietypublishing.org/ on January 16, 2018